

# Optically Active Transition Metal Complexes. 130.<sup>1</sup> Synthesis, Crystal Structures, and Catalytic Properties of Chiral-at-Metal ( $\eta^6$ -Arene)ruthenium(II) and ( $\eta^6$ -Arene)osmium(II) Half-Sandwich Complexes. Crystallization of Pure Diastereomers versus Diastereomer Mixtures in a 1:1 Ratio

Henri Brunner,\* Thomas Zwack, and Manfred Zabel†

*Institut für Anorganische Chemie, Universität Regensburg, D-93040 Regensburg, Germany*

Wolfgang Beck and Andreas Böhm

*Department Chemie, Ludwig-Maximilians-Universität, Butenandtstrasse 5-13,  
D-81377 München, Germany*

Received November 22, 2002

Condensation of a number of optically active amines and  $\alpha$ -amino acid esters with salicylaldehyde gave the chiral compounds **HLL**\*-**1**–**HLL**\*-**8**. A series of diastereomeric complexes of the type ( $R_M, S_C$ )- and ( $S_M, S_C$ )-[( $\eta^6$ -arene)M(LL\*)X] (**1**–**14**: M = Ru, Os; X = Cl, I), differing only in the metal configuration, were formed by reaction of [( $\eta^6$ -arene)MCl<sub>2</sub>]<sub>2</sub> with these compounds in the presence of base and by halogen exchange. Five of the complexes were characterized by X-ray structure analyses. Three cases showed the structural peculiarity that the single crystals contained the  $R_M, S_C$  and  $S_M, S_C$  diastereomers with opposite configurations at the metal centers in a 1:1 ratio, whereas two cases crystallized as pure  $R_M, S_C$  diastereomers. Two complexes, the ligands of which (the salicylaldimines of methyl phenylalaninate and methyl phenylglycinate) had racemized during the synthesis, crystallized as racemates  $R_{Ru}, S_C/S_{Ru}, R_C$ . Complexes **1**–**14** were tested as catalysts in the enantioselective isomerization of 2-*n*-butyl-4,7-dihydro-1,3-dioxepin to give 2-*n*-butyl-4,5-dihydro-1,3-dioxepin. Enantioselectivities up to 64% ee were achieved.

## Introduction

The catalytic potential of ruthenium complexes in organic synthesis is well documented.<sup>2</sup> Frequently, half-sandwich ( $\eta^6$ -arene)ruthenium(II) complexes have been used as precatalysts.<sup>3</sup> In such half-sandwich complexes of the three-legged piano-stool type, which contain the unsymmetrical chelate ligand LL' and another ligand X, e.g. a halide, the metal atom is a chiral center. Using an enantiomerically pure ligand LL\*, e.g. of  $S_C$  configuration, the two diastereomers  $R_M, S_C$  and  $S_M, S_C$  arise.<sup>4–6</sup> Many studies on chiral-at-metal ruthenium compounds of the type [( $\eta^6$ -arene)Ru(LL\*)L] and [( $\eta^6$ -arene)Ru(LL\*)L]X (arene = benzene, mesitylene, hexamethylbenzene, *p*-cymene, LL\* = anionic or neutral enantiomerically pure chelate ligand, L = monodentate ligand or halide, X = anion) have been reported, including

amino acid chelates,<sup>7,8</sup> and much fewer studies on analogous chiral-at-metal ( $\eta^6$ -arene)osmium compounds.

In the present paper we describe the synthesis and characterization as well as kinetic studies on the stability of the metal configuration of ruthenium(II) and osmium(II) half-sandwich complexes.<sup>9</sup> The main focus will be on two points: (i) their use in the enantioselective catalytic desymmetrization of 2-*n*-butyl-4,7-dihydro-1,3-dioxepin and (ii) the crystallization of the diastereomer mixtures. Concerning the second point, in the vast majority of cases single crystals obtained from the solution of a mixture of diastereomers contain only one diastereomer. This, actually, is the basis for the resolution of racemates by diastereomer separation via crystallization. There are, however, a few examples known with two diastereomers of the same ligand configuration and opposite metal configuration present in the same single crystal.<sup>10–20</sup> In the present study three of the new

\* To whom correspondence should be addressed. Fax: +49-941-9434439. E-mail: henri.brunner@chemie.uni-regensburg.de.

† X-ray structure analyses.

(1) Part 129: Brunner, H.; Klankermayer, J.; Zabel, M. *Organometallics* **2002**, *21*, 5746.

(2) Naota, T.; Takaya, H.; Murahashi, S.-I. *Chem. Rev.* **1998**, *98*, 2599.

(3) Noyori, R.; Hashiguchi, S. *Acc. Chem. Res.* **1997**, *30*, 97.

(4) Brunner, H. *Adv. Organomet. Chem.* **1980**, *18*, 151.

(5) Brunner, H. *Angew. Chem.* **1999**, *111*, 1248; *Angew. Chem., Int. Ed.* **1999**, *38*, 1194.

(6) Brunner, H. *Eur. J. Inorg. Chem.* **2001**, 905.

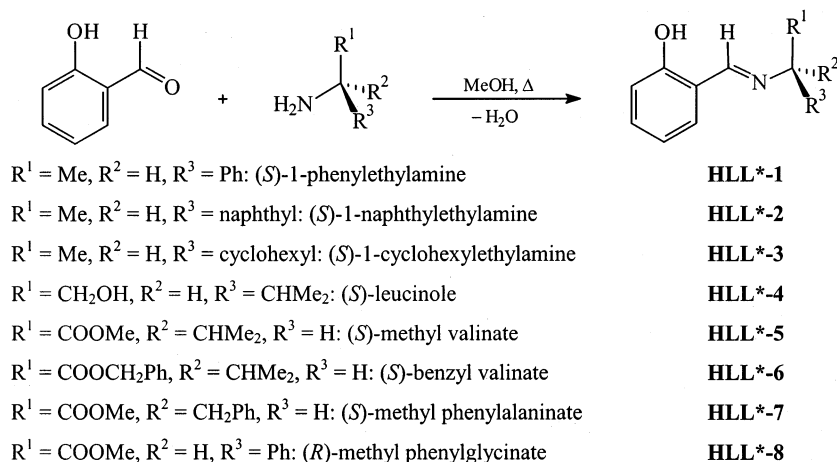
(7) Severin, K.; Berge, R.; Beck, W. *Angew. Chem.* **1998**, *110*, 1722; *Angew. Chem., Int. Ed.* **1998**, *37*, 1635.

(8) Carmona, D.; Lamata, M. P.; Oro, L. A. *Eur. J. Inorg. Chem.* **2002**, 2239.

(9) Zwack, T., Ph.D. Thesis, Universität Regensburg, 2001.

(10) Krämer, R.; Polborn, K.; Wanjek, H.; Zahn, I.; Beck, W. *Chem. Ber.* **1990**, *123*, 767; Krämer, R.; Maurus, M.; Polborn, K.; Sünkel, K.; Robl, C.; Beck, W. *Chem. Eur. J.* **1996**, *2*, 1518.

(11) Carmona, D.; Mendoza, A.; Lahoz, F. J.; Oro, L. A.; Lamata, M. P.; San José, E. *J. Organomet. Chem.* **1990**, *396*, C17.

**Scheme 1. Synthesis of the Optically Active Salicylaldiminates HLL\*-1–HLL\*-8**

complexes showed the structural peculiarity of a 1:1 diastereomer crystallization including a ruthenium complex, the corresponding intimately related osmium compound of which did not show 1:1 diastereomer crystallization but crystallization as a pure diastereomer in two different modifications, indicating a delicate balance between the 1:1 diastereomer crystallization and the crystallization as a pure diastereomer. This alternative, of fundamental importance for optical resolutions by diastereomer separation via crystallization, will be analyzed.

**Results and Discussion**

**Syntheses.** Compounds **HLL\*-1–HLL\*-8** were prepared by condensation of salicylaldehyde with the appropriate chiral amines or amino acid esters in methanol by gentle heating. **HLL\*-1–HLL\*-4** were condensation products of commercially available chiral amines and salicylaldehyde. **HLL\*-5–HLL\*-8** were Schiff bases of salicylaldehyde and  $\alpha$ -amino acid esters. The synthesis of the optically active salicylaldiminates is shown in Scheme 1. As the amino acid derived compounds **HLL\*-5–HLL\*-8** could have racemized during the synthesis,<sup>21</sup> they were examined by <sup>1</sup>H NMR spectroscopy with (*S*)-(+)-1-(9-anthryl)-2,2,2-trifluoroethanol. **HLL\*-5** turned out to be enantiomerically pure even when strong bases had been used. However, the phenylalanine derivative **HLL\*-7** could be obtained enantiomerically pure only with weak bases such as NaHCO<sub>3</sub>. **HLL\*-8** was isolated with 60% ee under conditions for which no racemization had been reported.<sup>22</sup>

For the synthesis of diastereomeric ruthenium and osmium complexes **1–14**, the ligands were dissolved in

methylene chloride and deprotonated using KO<sup>t</sup>Bu. After the suspension was cooled to  $-78\text{ }^\circ\text{C}$ ,  $[(\eta^6\text{-arene})\text{-MCl}_2]$  (arene = benzene, mesitylene, hexamethylbenzene, *p*-cymene; M = Ru, Os) was added (Schemes 2 and 3). Complexes **1**<sup>12,23</sup> and **9**<sup>24,25</sup> were known. Complex **14** was formed by halogen exchange using complex **5** and an excess of sodium iodide in methanol.

All the complexes **1–14** contained enantiomerically pure *S*-configured ligands, except complexes **7** and **8**, the ligands of which had completely racemized during complex formation. Thus, in solution all the complexes consisted of the two diastereomers  $R_M, S_C$  and  $S_M, S_C$ , differing only in the metal configuration, except complexes **7** and **8**, for which two diastereomeric pairs of enantiomers,  $R_M, S_C/S_M, R_C$  and  $S_M, S_C/R_M, R_C$ , were present—a stereochemical situation similar but not identical with the two diastereomers  $R_M, S_C$  and  $S_M, S_C$ .

**Diastereomer Equilibria and Epimerization Studies.** For all the complexes **1–14** the diastereomers  $R_M, S_C$  and  $S_M, S_C$ , which only differ in the configuration at the metal center, exhibited different <sup>1</sup>H NMR spectra. Thus, the diastereomer ratio could be determined by integration of suitable signals. In the majority of the present ( $\eta^6\text{-arene}$ )ruthenium and ( $\eta^6\text{-arene}$ )osmium complexes the signals of the  $\eta^6\text{-arene}$  ligand of the major diastereomer showed a high-field shift compared to those of the minor diastereomer. Such a behavior also had been observed for other half-sandwich complexes subject to the “ $\beta$ -phenyl effect”.<sup>26</sup> This  $\beta$ -phenyl effect is an attractive C–H/ $\pi$ -interaction<sup>27</sup> present only in the major diastereomers. It arises because, by rotation about the N–C\* and C\*–C<sub>ipso</sub> bonds of the 1-phenylethyl group, the phenyl substituent moves as close to the  $\pi$ -bonded arene ligand as possible (T-shaped arrangement of the phenyl and the arene ligand). Due to this face-on orientation, the arene ligand lies in the magnetic anisotropy cone of the phenyl ring of the

(12) Mandal, S. K.; Chakravarty, A. R. *J. Chem. Soc., Dalton Trans.* **1992**, 1627.

(13) Mandal, S. K.; Chakravarty, A. R. *Inorg. Chem.* **1993**, *32*, 3851.

(14) Carter, L. C.; Davies, D. L.; Duffy, K. T.; Fawcett, J.; Russel, D. R. *Acta Crystallogr., Sect. C* **1994**, *50*, 1559.

(15) Attar, S.; Catalano, V. J.; Nelson, J. H. *Organometallics* **1996**, *15*, 2932.

(16) Brunner, H.; Neuhierl, T.; Nuber, B. *Eur. J. Inorg. Chem.* **1998**, 1877.

(17) Faller, J. W.; Liu, X.; Parr, J. *Chirality* **2000**, *12*, 325.

(18) Rath, R. K.; Nethanji, M.; Chakravarty, A. R. *Polyhedron* **2002**, *21*, 1929.

(19) Brunner, H.; Weber, M.; Zabel, M. *Synthesis*, in press.

(20) Brunner, H.; Dormeier, S.; Zabel, M. *Eur. J. Inorg. Chem.* **2002**, 2594.

(21) Grigg, R.; Gunaratne, H. Q. N. *Tetrahedron Lett.* **1983**, *24*, 4457 and literature cited therein.

(22) Fuhrhop, J.; Penzlin, G. *Organic Synthesis*, 2nd ed.; VCH: Weinheim, Germany, 1994; p 232.

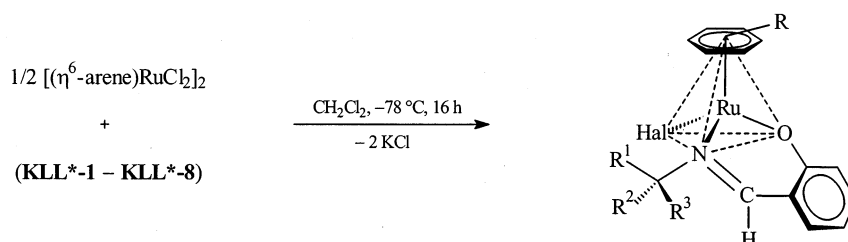
(23) Mandal, S. K.; Chakravarty, A. R. *J. Organomet. Chem.* **1991**, *417*, C59.

(24) Brunner, H.; Oeschey, R.; Nuber, B. *Angew. Chem.* **1994**, *106*, 941; *Angew. Chem., Int. Ed. Engl.* **1994**, *33*, 866.

(25) Brunner, H.; Oeschey, R.; Nuber, B. *J. Chem. Soc., Dalton Trans.* **1996**, 1499.

(26) Brunner, H. *Angew. Chem.* **1983**, *95*, 921; *Angew. Chem., Int. Ed. Engl.* **1983**, *22*, 897 and literature cited therein.

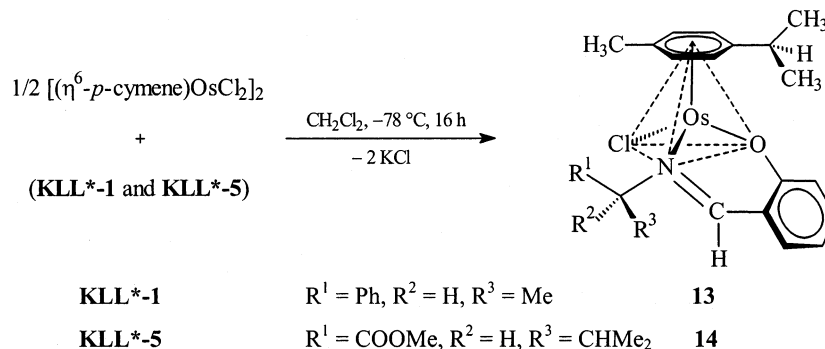
(27) Nishio, M.; Hirota, M.; Umezawa, Y. *The CH/ $\pi$  Interaction*; Wiley-VCH: Weinheim, Germany, 1998.

Scheme 2. Synthesis of the Half-Sandwich Ruthenium(II) Complexes 1–12<sup>a</sup>

Ar = <i>p</i> -cymene, R <sup>1</sup> = Ph, R <sup>2</sup> = H, R <sup>3</sup> = Me	Hal = Cl	1
Ar = <i>p</i> -cymene, R <sup>1</sup> = naphthyl, R <sup>2</sup> = H, R <sup>3</sup> = Me	Hal = Cl	2
Ar = <i>p</i> -cymene, R <sup>1</sup> = cyclohexyl, R <sup>2</sup> = H, R <sup>3</sup> = Me	Hal = Cl	3
Ar = <i>p</i> -cymene, R <sup>1</sup> = CH <sub>2</sub> OH, R <sup>2</sup> = H, R <sup>3</sup> = CHMe <sub>2</sub>	Hal = Cl	4
Ar = <i>p</i> -cymene, R <sup>1</sup> = COOMe, R <sup>2</sup> = H, R <sup>3</sup> = CHMe <sub>2</sub>	Hal = Cl	5
Ar = <i>p</i> -cymene, R <sup>1</sup> = COOCH <sub>2</sub> Ph, R <sup>2</sup> = H, R <sup>3</sup> = CHMe <sub>2</sub>	Hal = Cl	6
Ar = <i>p</i> -cymene, R <sup>1</sup> = COOMe, R <sup>2</sup> = H, R <sup>3</sup> = CH <sub>2</sub> Ph	Hal = Cl	7
Ar = <i>p</i> -cymene, R <sup>1</sup> = COOMe, R <sup>2</sup> = H, R <sup>3</sup> = Ph	Hal = Cl	8
Ar = benzene, R <sup>1</sup> = Ph, R <sup>2</sup> = H, R <sup>3</sup> = Me	Hal = Cl	9
Ar = mesitylene, R <sup>1</sup> = Ph, R <sup>2</sup> = H, R <sup>3</sup> = Me	Hal = Cl	10
Ar = hexamethylbenzene, R <sup>1</sup> = Ph, R <sup>2</sup> = H, R <sup>3</sup> = Me	Hal = Cl	11
Ar = <i>p</i> -cymene, R <sup>1</sup> = COOMe, R <sup>2</sup> = H, R <sup>3</sup> = CHMe <sub>2</sub>	Hal = I	12

<sup>a</sup> For **1–11** only the diastereomers with the *R*<sub>Ru</sub>,*S*<sub>C</sub> configuration are shown; for **12** only the diastereomer with the *S*<sub>Ru</sub>,*S*<sub>C</sub> configuration is shown.

## Scheme 3. Synthesis of the Half-Sandwich Osmium(II) Complexes 13 and 14



<sup>a</sup> Only the diastereomer with the *R*<sub>Os</sub>,*S*<sub>C</sub> configuration is shown.

1-phenylethyl substituent, which causes the high-field shift. In the solid state this face-on orientation is found in complexes **1**,<sup>23</sup> **2**, and **13** (see below).

It is known that the β-phenyl effect persists in solution.<sup>26</sup> It is responsible for the high-field shift of the signal of the major diastereomer compared to the minor diastereomer, the signal of which appears at its normal position. The β-phenyl effect also affects the diastereomer ratios at equilibrium, the major diastereomer being favored by the attractive C–H/π-interaction with respect to the minor diastereomer. For ruthenium complex **1** the ratio in CDCl<sub>3</sub> was *R*<sub>Ru</sub>,*S*<sub>C</sub>:*S*<sub>Ru</sub>,*S*<sub>C</sub> = 85:15,<sup>13,23</sup> and for the osmium analogue it was 80:20. Going from the phenyl to a naphthyl substituent in the 1-arylethyl group in the Ru series increased the diastereomer ratio at equilibrium. Thus, for the 1-naphthyl complex **2** only one diastereomer was observed, indicating a diastereomer ratio > 99:1. The assignment of the *R*<sub>Ru</sub>,*S*<sub>C</sub> configuration to the dominating isomer was supported by the high-field shift of the η<sup>6</sup>-*p*-cymene signal in the <sup>1</sup>H NMR spectrum. If the attractive

intramolecular C–H/π-interaction was lacking, the equilibrium diastereomer ratios dropped to unspectacular values around 50:50. Thus, the cyclohexyl ring of ligand **HLL**\*-3 in complex **3** did not interact with the cymene ligand, the diastereomer ratio in CDCl<sub>3</sub> being 54:46.

The equilibrium diastereomer ratios for the chloro- and iodoruthenium complexes **5** and **12**, in CDCl<sub>3</sub> containing the valine methyl ester ligand, were 70:30; for the osmium complex **14**, the analogue of **5**, it was 64:36. The ratio increased for the benzyl ester **6** and the benzyl derivative **7** to 80:20. The rise of the diastereomer excess to 84% de in complex **8** may be due to a C–H/π-interaction.

In the solid state diastereomers such as those discussed here are configurationally stable at the metal atom. In solution some of them prove to be stable; others are labile with respect to the metal configuration.<sup>4–6</sup> Knowledge of the configurational stability is important, as the lability of the metal configuration has been overlooked in a number of recent papers, resulting in

misinterpretations and wrong conclusions.<sup>6,28</sup> Low-temperature <sup>1</sup>H NMR is a convenient tool for studying the configurational stability/lability at the metal atom.

( $\eta^6$ -Arene)ruthenium half-sandwich complexes of the type **1–11** have been studied with respect to the stability of the metal configuration in detailed kinetic studies<sup>24,25,29</sup> which showed that the epimerization is already rapid at temperatures below room temperature. Thus, solutions of ruthenium complexes **1–11**, standing for some time at room temperature, will contain the two diastereomers  $R_{Ru,S_C}$  and  $S_{Ru,S_C}$  at their equilibrium concentrations.

To investigate the configurational stability of the corresponding osmium complexes, powdered crystals of ( $R_{Os,S_C}$ )-**14** were dissolved in CD<sub>2</sub>Cl<sub>2</sub> at  $-60$  °C, <sup>1</sup>H NMR mainly showing the signals of the major diastereomer. The signals of the minor diastereomer were visible, albeit in a much lower concentration than at equilibrium. The presence of the signals of the minor diastereomer may be due to the start of epimerization during dissolution or, more probable, to the presence of small amounts of the minor diastereomer in the solid sample. Around  $-20$  °C the signals of the minor diastereomer grew until the diastereomer ratio had reached the equilibrium ratio 65:35, indicating that the configurational lability of the osmium compounds is similar to that of the corresponding ruthenium complexes.

**X-ray Structure Analyses.** In the present study we carried out eight X-ray structure analyses using crystals obtained from solutions of the various diastereomer mixtures. From solutions of the two diastereomers  $R_{M,S_C}$  and  $S_{M,S_C}$  in the three cases **5**, **12**, and **13**, unexpectedly, we found crystals which contained both diastereomers  $R_{M,S_C}$  and  $S_{M,S_C}$  in a 1:1 ratio in the same lattice. In the three cases **2** and **14** (two modifications of the latter species) we found the expected crystallization of a pure diastereomer, here of the favored  $R_{M,S_C}$  diastereomers. In the two cases **7** and **8** the ligands had racemized during the synthesis. Therefore, in solution the enantiomers of each of the two diastereomers  $R_{M,S_C}/S_{M,R_C}$  and  $S_{M,S_C}/R_{M,R_C}$  were present. In these two cases the enantiomers of the major diastereomer  $R_{Ru,S_C}/S_{Ru,R_C}$  crystallized.

1:1 diastereomer crystallization as encountered in the cocrystallization of the diastereomers  $R_{M,S_C}$  and  $S_{M,S_C}$  of **5**, **12**, and **13** is most unusual, because normally the crystallization of a diastereomer mixture gives single crystals of one diastereomer, usually the less soluble diastereomer, which in fact is the basis for the resolution of racemates by conversion into diastereomers and separation via fractional crystallization.

The peculiar 1:1 cocrystallization of the two diastereomers  $R_{M,S_C}$  and  $S_{M,S_C}$  in one single crystal, discussed in a preliminary communication,<sup>30</sup> compared to the "normal" crystallization of one diastereomer ( $R_{M,S_C}$ ), has been analyzed for the intimately related compounds **5** and **14**, differing only in the central metal Ru and Os, respectively. In both compounds the asymmetric carbon atom in the ligand has the expected  $S_C$  configuration.

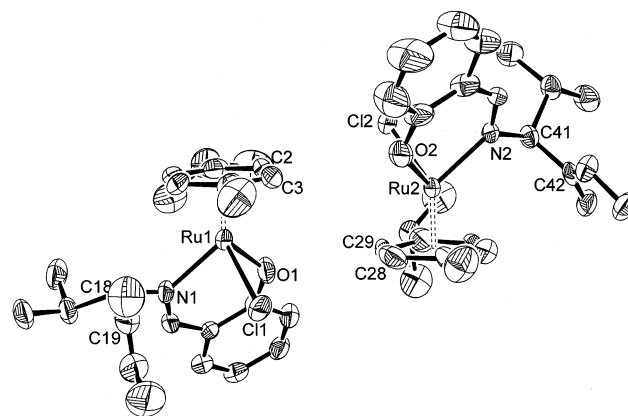


**Figure 1.** ORTEP plot of the molecular structure of complexes ( $R_{Ru,S_C}$ )-**5** (right side) and ( $S_{Ru,S_C}$ )-**5** (left side) in a 1:1 ratio within the same single crystal. Ellipsoids are drawn at the 50% probability level. Hydrogen atoms have been omitted for clarity.

**Table 1.** Bond Lengths (Å) and Angles (deg) in the 1:1 Lattice of ( $R_{Ru,S_C}$ )-**5** and ( $S_{Ru,S_C}$ )-**5** as Well as in the Monoclinic and Orthorhombic Modifications of ( $R_{Os,S_C}$ )-**14**

	( $R_{Ru,S_C}$ )- and ( $S_{Ru,S_C}$ )- <b>5</b> monoclinic	( $R_{Os,S_C}$ )- <b>14</b>	
		mono- clonic	ortho- rhombic
<b>Bond Lengths</b>			
M–Cy(centroid)	1.670–1.689	1.655	1.662
M–Cl	2.446(2)–2.423(2)	2.433(17)	2.4326(11)
M–O	2.062(6)–2.053(6)	2.077(5)	2.060(3)
M–N	2.092(6)–2.120(6)	2.101(5)	2.111(3)
<b>Bond Angles</b>			
O–M–Cl	85.15(19)–84.43(18)	84.02(14)	83.47(10)
N–M–Cl	82.94(18)–85.17(17)	83.98(15)	84.13(10)
O–M–N	88.6(2)–88.8(2)	87.3(3)	87.03(13)
<b>Dihedral Angle C(COOR)–C*–N–M</b>			
C42–C41–N2–Ru2	–83.6(6) <sup>a</sup>		
C19–C18–N1–Ru1	–76.1(7) <sup>b</sup>		
C2–C1–N–Os		–99.4(6)	

<sup>a</sup>  $R_{Ru,S_C}$  diastereomer. <sup>b</sup>  $S_{Ru,S_C}$  diastereomer.

The metal configuration is assigned according to the priority sequence Cy > Cl > O > N.<sup>31,32</sup>

Crystallization at 4 °C by diffusion of petroleum ether into a toluene solution of the two diastereomers ( $R_{Ru,S_C}$ )- and ( $S_{Ru,S_C}$ )-[( $\eta^6$ -*p*-cymene)Ru(LL\*)Cl] of **5** afforded dark red single crystals which contained two independent molecules in the ratio 1:1 in the unit cell. In both molecules the chiral carbon atoms of the valine ester groups had the expected  $S_C$  configuration, whereas ruthenium atom Ru1 had the  $R_{Ru}$  and ruthenium atom Ru2 the  $S_{Ru}$  configuration. Thus, from a 70:30 mixture in solution the two diastereomers  $R_{Ru,S_C}$  and  $S_{Ru,S_C}$  crystallized in a 1:1 ratio in the same single crystal (Figure 1).

In the 1:1 crystal of the two diastereomers of **5**, the bond lengths and bond angles of the two diastereomers  $R_{Ru,S_C}$  and  $S_{Ru,S_C}$  are relatively similar (Table 1). In the complex with  $S_{Ru}$  configuration the Ru–N and the Ru–Cy(centroid) distances are a little shorter, whereas the Ru–O and the Ru–Cl bonds are slightly longer than in the isomer with  $R_{Ru}$  configuration. Furthermore, two

(28) Brunner, H.; Zwack, T. *Organometallics* **2000**, *19*, 2423.

(29) Brunner, H.; Oeschey, R.; Nuber, B. *Inorg. Chem.* **1995**, *34*, 3349.

(30) Brunner, H.; Weber, M.; Zwack, T.; Zabel, M. Submitted for publication in *Angew. Chem.*

(31) Lecomte, C.; Dusausoy, Y.; Protas, J.; Tirouflet, J.; Dormond, A. *J. Organomet. Chem.* **1974**, *73*, 67.

(32) Brunner, H. *Enantiomer* **1997**, *2*, 133.

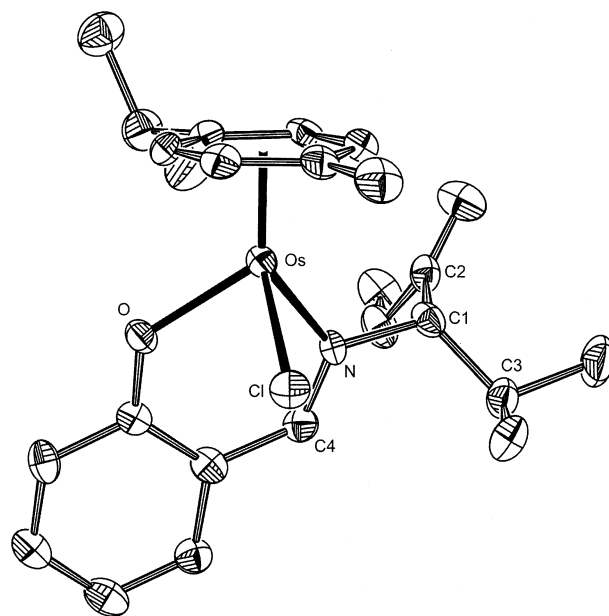
bond angles are smaller and one is larger, but only slightly, emphasizing the similarity between the two diastereomers. The ester substituent at the chiral carbon atom in both cases is almost perpendicular to the chelate plane (dihedral angles  $-83.6$  and  $-76.1^\circ$ ). In the  $S_{Ru}, S_C$  isomer it orients toward the chloro ligand, whereas in the  $R_{Ru}, S_C$  isomer it points toward the cymene ligand.

Figure 1 shows that the two diastereomers almost form a "racemate", connected by an "inversion center". In our analysis we place this inversion center exactly halfway between Ru1 and Ru2. The deviations of the four different substituents around the Ru atoms, Cy (centroid), Cl, O, and N, from inversion symmetry are extremely small, ranging between 0.13 and 0.23 Å. Similarly, the atoms in the ligand backbones and in the cymene rings facing each other closely follow this inversion symmetry with deviations below 0.2 Å. Naturally, inconsistencies arise for the chiral nitrogen substituents, which for both diastereomers have the same *S* configuration, excluding inversion symmetry.

At 5.6420(9) Å the Ru–Ru distance in the "inversion pair" is extremely short. All the other Ru–Ru distances are longer than 8.6 Å. Thus, in these inversion pairs two diastereomers assemble in the same way as two enantiomers do in a racemate related by an inversion center, forming a kind of supramolecular aggregate on the basis of molecular recognition. In the center the pairs of diastereomers  $R_{Ru}, S_C$  and  $S_{Ru}, S_C$  are image/mirror image related; toward the outside of the pairs, however, centrosymmetry is lost. The lattice is formed by translation of these inversion pairs.

In the 1:1 crystals of ( $R_{Ru}, S_C$ )-**5**/( $S_{Ru}, S_C$ )-**5** molecular recognition occurs between two (Cy)Ru(O<sub>sal</sub>)Cl fragments of opposite metal configuration, which approach each other by inversion symmetry. With almost parallel Ru–Cy centroids the fragments orient their O<sub>sal</sub>–Cl edges toward one another, resulting in O1–Cl2 and O2–Cl1 distances of 5.174 and 5.352 Å. There are 2 × 2 hydrogen bonds between the C–H groups of the cymene rings and the Cl and O<sub>sal</sub> substituents of opposite molecules (distances (angles) C3–H···O2 = 3.467 Å (163.41°), C29–H···O1 = 3.307 Å (170.87°), C2–H···Cl2 = 3.656 Å (143.93°), and C28–H···Cl1 = 3.742 Å (141.15°)), which arrange the isopropyl and methyl groups of the cymene rings such that together with the chloro and the oxygen substituents they close a shell around the inner core of the inversion pair.

Osmium complex **14**, the analogue of ruthenium complex **5**, is also configurationally labile in solution. The diastereomer ratio in CDCl<sub>3</sub> at room temperature is 64:36, similar to that for the corresponding ruthenium complex. Diffusion of petroleum ether into a toluene solution of **14** affords two different types of red crystals, both suitable for X-ray analysis. Both contain only the  $R_{Os}, S_C$  diastereomer in the monoclinic and orthorhombic system, respectively. Thus, surprisingly, the osmium compound **14** crystallizes as a pure diastereomer and not as a 1:1 mixture of two diastereomers (Figure 2). The relevant bond lengths and angles for both modifications are given in Table 1 (last two columns). They are extremely similar to those of the two ruthenium diastereomers. This is a consequence of the well-known lanthanide contraction, which makes the radii of Ru and



**Figure 2.** ORTEP plot of the molecular structure of the complex ( $R_{Os}, S_C$ )-**14** (monoclinic modification). Ellipsoids are drawn at the 50% probability level. Hydrogen atoms have been omitted for clarity.

Os almost the same. Thus, some of the Os–ligand bonds and ligand–Os–ligand angles are slightly shorter and some are slightly longer than in the two ruthenium diastereomers. Some are even intermediate between those of the two ruthenium diastereomers.

In the crystal of ( $R_{Os}, S_C$ )-**14** the ester substituent is almost perpendicular to the chelate plane and oriented toward the cymene ligand similar to the  $R_{Ru}, S_C$  diastereomer. Given the extreme similarities between the diastereomers ( $R_{Ru}, S_C$ )- and ( $S_{Ru}, S_C$ )-**5** and ( $R_{Os}, S_C$ )- and ( $S_{Os}, S_C$ )-**14** it is surprising that the ruthenium complexes crystallize as two diastereomers in a 1:1 ratio, while in the osmium case a single diastereomer crystallizes, even in two different modifications. This shows that there is a delicate balance between the two situations: crystallization as a pure diastereomer or crystallization as two diastereomers in a 1:1 ratio. Taking into account on one hand the similarity of the Ru and Os diastereomers **5** and **14** and on the other hand their different behaviors on crystallization, the conclusion is that it will be difficult to predict which of the two alternatives will be realized in other cases.

In both modifications of **14** the diastereomer ( $R_{Os}, S_C$ )-**14** forms the lattice with the shortest Os–Os distance, 8.1771(6) Å. There are no metal–metal distances around 5.6 Å as in the 1:1 ruthenium "inversion pairs". All the Os–Os distances are in the range of the Ru–Ru distances outside the "inversion pairs".

As for complex **5**, 1:1 cocrystallization of the two diastereomers  $R_M, S_C/S_M, S_C$  was also observed for the iodoruthenium complex **12** and for the (*S*)-1-phenylethyl-derived osmium complex **13**. These cases were analyzed similarly to those of the 1:1 crystal of complex **5**. Thus, the Ru–Ru distance of 5.8194(19) Å in the inversion pair of the iodo complex was much smaller than the outside-pair Ru–Ru distances, which only started at 7.4221(18) Å. The 1:1 diastereomer cocrystallization of the Os complex **13** closely linked up with that of its Ru

**Table 2. Crystallographic Data for Compounds 5, 12, and 13**

	<b>5</b>	<b>12</b>	<b>13</b>
empirical formula	2 × C <sub>23</sub> H <sub>30</sub> ClNO <sub>3</sub> Ru	2 × C <sub>25</sub> H <sub>28</sub> ClNOOs	2 × C <sub>23</sub> H <sub>30</sub> ClNO <sub>3</sub> Ru
fw	2 × 505.02	2 × 584.16	2 × 596.45
cryst syst	monoclinic	monoclinic	triclinic
space group	<i>P2</i> <sub>1</sub>	<i>P2</i> <sub>1</sub>	<i>P1</i>
<i>Z</i>	2	4	2
<i>a</i> (Å)	11.4964(10)	10.9275(9)	7.9952(7)
<i>b</i> (Å)	16.0597(9)	16.8397(11)	10.1954(12)
<i>c</i> (Å)	12/86028(11)	12.79449(10)	15.0628(14)
α (deg)	90	90	77.111(12)
β (deg)	106.889(9)	110.506(9)	86.246(11)
γ (deg)	90	90	88.921(12)
<i>V</i> (Å <sup>3</sup> )	2272.0(3)	2205.2(3)	1194.3(2)
ρ <sub>calcd</sub> (g cm <sup>-3</sup> )	1.476	1.760	1.659
abs coeff (mm <sup>-1</sup> )	0.831	5.920	1.971
<i>F</i> (000)	1040	1144	592
θ range (deg)	2.24–25.86	1.99–25.77	2.05–25.87
no. of rflns	31 852	31 086	9954
<i>R</i> <sub>int</sub>	–0.0346	0.0909	0.0827
no. of data/params	8673/523	8373/523	6061/293
goodness of fit on <i>F</i> <sup>2</sup>	1.113	1.061	1.069
R1/wR2 ( <i>I</i> > 2σ( <i>I</i> ))	0.0548/0.1378	0.0272/0.0649	0.0632/0.1840
R1/wR2 (all data)	0.0595/0.1407	0.0284/0.0652	0.0744/0.1913
largest diff peak and hole (e Å <sup>-3</sup> )	3.429/–0.987	2.057/–1.481	0.993/–1.239
CCDC no.	193233	193238	193232

**Table 3. Crystallographic Data for Compounds 2, 7, 8, and 14**

	<b>2</b>	<b>7</b>	<b>8</b>	<b>14</b>	
empirical formula	C <sub>29</sub> H <sub>30</sub> ClNORu	C <sub>27</sub> H <sub>30</sub> ClNO <sub>3</sub> Ru	C <sub>26</sub> H <sub>28</sub> ClNO <sub>3</sub> Ru	C <sub>23</sub> H <sub>30</sub> ClNO <sub>3</sub> Os	C <sub>23</sub> H <sub>30</sub> ClNO <sub>3</sub> Os
fw	545.86	553.04	539.01	594.16	594.16
cryst syst	orthorhombic	orthorhombic	triclinic	monoclinic	orthorhombic
space group	<i>P2</i> <sub>1</sub> <i>2</i> <sub>1</sub> <i>2</i> <sub>1</sub>	<i>Pbca</i>	<i>P1</i>	<i>P2</i> <sub>1</sub>	<i>P2</i> <sub>1</sub> <i>2</i> <sub>1</sub> <i>2</i> <sub>1</sub>
<i>Z</i>	4	8	2	2	4
<i>a</i> (Å)	11.1932(6)	7.7043(3)	7.9845(9)	9.3664(7)	8.6386(5)
<i>b</i> (Å)	12.3356(6)	18.5592(7)	11.2624(11)	15.8032(11)	15.5224(11)
<i>c</i> (Å)	38.174(2)	34.0149(19)	13.9219(15)	9.0952(7)	16.8700(11)
α (deg)	90	90	100.291(12)	90	90
β (deg)	90	90	103.497(12)	123.299(8)	90
γ (deg)	90	90	98.144(12)	90	90
<i>V</i> (Å <sup>3</sup> )	–5270.9(5)	4863.6(4)	1175.6(2)	1125.23(18)	2262.1(3)
ρ <sub>calcd</sub> (g cm <sup>-3</sup> )	1.482	1.511	1.523	1.754	1.745
abs coeff (mm <sup>-1</sup> )	0.82	0.784	0.808	5.808	5.778
<i>F</i> (000)	2412	2272	552	584	1168
θ range (deg)	1.73–25.18	2.27–25.22	2.67–25.77	2.51–25.75	2.62–25.83
no. of rflns	57 390	47 485	16 425	11 588	22 009
<i>R</i> <sub>int</sub>	0.0507	0.0802	0.0741	0.0379	0.0826
no. of data/params	9259/622	4366/298	4180/289	4201/262	4338/262
goodness of fit on <i>F</i> <sup>2</sup>	1.012	1.049	0.999	1.019	1.043
R1/wR2 ( <i>I</i> > 2σ( <i>I</i> ))	0.0290/0.0676	0.0361/0.0898	0.0284/0.0694	0.0245/0.0562	0.0241/0.0568
R1/wR2 (all data)	0.0349/0.0699	0.0463/0.0941	0.0349/0.0713	0.0284/0.0570	0.0251/0.0570
largest diff peak and hole (e Å <sup>-3</sup> )	0.827/–0.401	0.992/–0.811	0.971/–0.608	1.948/–1.110	1.668/–1.265
CCDC no.	193231	193235	193234	193236	193237

counterpart.<sup>12</sup> The crystallographic data of **5**, **12**, and **13** are summarized in Table 2.

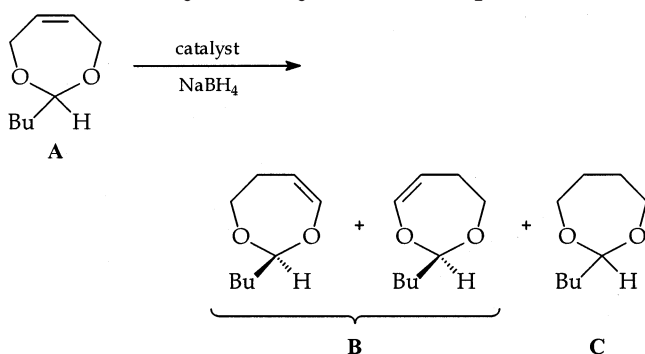
1:1 cocrystallization of two diastereomers in the same lattice has been observed occasionally.<sup>20</sup> Interestingly, the phenomenon is frequently encountered in the crystallization of chiral-at-metal (*η*<sup>6</sup>-arene)ruthenium complexes of the three-legged piano-stool type from solutions containing both diastereomers. The first examples were reported in 1990<sup>10,11</sup> and 1992.<sup>12</sup> Examples from other groups<sup>14,15,17,18</sup> and our own group<sup>16</sup> followed. Three new examples are part of the present paper, and another example will be published elsewhere.<sup>19</sup> Interestingly, the basis for most of these 1:1 diastereomer cocrystallizations is the molecular recognition motif found for (*R*<sub>Ru</sub>,*S*<sub>C</sub>)-**5**/(*S*<sub>Ru</sub>,*S*<sub>C</sub>)-**5**, as discussed in ref 30. Of course, many (*η*<sup>6</sup>-arene)ruthenium complexes also crystallize “normally” as pure diastereomers from solutions containing diastereomer mixtures, as do complexes **2** and **14**.

Complex **2** crystallized as the pure *R*<sub>Ru</sub>,*S*<sub>C</sub> diastereomer similar to compound **14**. The 1-naphthyl substituent showed a face-on orientation toward the cymene ligand (see above). The crystallographic data of **2** and **14** are summarized in Table 3 together with the corresponding data for **7** and **8**, the crystals of which contain the enantiomers *R*<sub>Ru</sub>,*S*<sub>C</sub>/*S*<sub>Ru</sub>,*R*<sub>C</sub> of the major diastereomer—an expected behavior for the stereochemical situation given. In the unit cell of crystals of **7** there are eight molecules which subdivide into two mirror image related four-molecule groups.<sup>9</sup>

The <sup>1</sup>H NMR spectra of 1:1 crystals of **5**, **12**, and **13**, dissolved in CD<sub>2</sub>Cl<sub>2</sub> at –80 °C, showed a ratio of the two diastereomers of exactly 50:50, the composition of the crystals. Similarly prepared solutions of **2**, **7**, **8**, and **14**, containing only one diastereomer or the enantiomers of one diastereomer, exhibited only one set of signals. When these solutions were warmed to room temperature, all the ratios changed to the corresponding equi-

**Table 4. Enantioselective Desymmetrization of 2-*n*-Butyl-4,7-dihydro-1,3-dioxepin (A) according to Scheme 4**

entry	catalyst	yield (%)		ee of B (%)
		B	C	
1	$[(\eta^6\text{-}p\text{-cymene})\text{Ru}(\text{LL}^*\text{-1})\text{Cl}]$ ( <b>1</b> )	99.2, 99.1	0.8, 0.9	51.0, 50.7 (+)
2	$[(\eta^6\text{-benzene})\text{Ru}(\text{LL}^*\text{-1})\text{Cl}]$ ( <b>9</b> )	31.2, 31.1	14.1, 15.5	4.3, 4.7 (+)
3	$[(\eta^6\text{-mesitylene})\text{Ru}(\text{LL}^*\text{-1})\text{Cl}]$ ( <b>10</b> )	11.4, 10.8	1.0, 1.1	20.4, 19.6 (+)
4	$[(\eta^6\text{-C}_6\text{Me}_6)\text{Ru}(\text{LL}^*\text{-1})\text{Cl}]$ ( <b>11</b> )	1.0, 1.5	0.5, 0.7	3.3, 3.6 (+)
5	$[(\eta^6\text{-}p\text{-cymene})\text{Ru}(\text{LL}^*\text{-2})\text{Cl}]$ ( <b>2</b> )	95.3, 94.3	1.4, 1.0	53.5, 52.3 (+)
6	$[(\eta^6\text{-}p\text{-cymene})\text{Ru}(\text{LL}^*\text{-3})\text{Cl}]$ ( <b>3</b> )	97.4, 97.6	2.5, 2.3	55.7, 54.5 (+)
7	$[(\eta^6\text{-}p\text{-cymene})\text{Ru}(\text{LL}^*\text{-4})\text{Cl}]$ ( <b>4</b> )	11.9, 15.6	1.1, 1.3	2.0, 3.1 (+)
8	$[(\eta^6\text{-}p\text{-cymene})\text{Ru}(\text{LL}^*\text{-5})\text{Cl}]$ ( <b>5</b> )	98.2, 98.3	1.7, 1.6	64.3, 64.3 (-)
9	$[(\eta^6\text{-}p\text{-cymene})\text{Ru}(\text{LL}^*\text{-5})\text{I}]$ ( <b>12</b> )	97.9, 97.7	2.0, 2.3	63.8, 59.9 (-)
10	$[(\eta^6\text{-}p\text{-cymene})\text{Ru}(\text{LL}^*\text{-6})\text{Cl}]$ ( <b>6</b> )	98.3, 97.7	1.6, 2.1	48.6, 48.6 (-)
11	$[(\eta^6\text{-}p\text{-cymene})\text{Ru}(\text{LL}^*\text{-7})\text{Cl}]$ ( <b>7</b> )	97.0, 97.0	1.5, 1.2	
12	$[(\eta^6\text{-}p\text{-cymene})\text{Ru}(\text{LL}^*\text{-8})\text{Cl}]$ ( <b>8</b> )	63.0, 62.7	2.7, 1.6	
13	$[(\eta^6\text{-}p\text{-cymene})\text{Os}(\text{LL}^*\text{-1})\text{Cl}]$ ( <b>13</b> )	46.3, 46.4	1.3, 0.6	0.3, 0.1 (-)
14	$[(\eta^6\text{-}p\text{-cymene})\text{Os}(\text{LL}^*\text{-5})\text{Cl}]$ ( <b>14</b> )	75.2, 75.8	0.9, 0.7	0.2, 0.2 (-)

**Scheme 4. Enantioselective Isomerization of 2-*n*-Butyl-4,7-dihydro-1,3-dioxepin (A)**

librium concentrations of the diastereomers, as addressed in the previous paragraph.<sup>9</sup>

**Catalytic Studies.** Complexes **1–14** were used as catalysts in the enantioselective double bond migration in 2-*n*-butyl-4,7-dihydro-1,3-dioxepin (A) to give 2-*n*-butyl-4,5-dihydro-1,3-dioxepin (B) (Scheme 4), which is a precursor for the syntheses of natural products.<sup>33,35</sup> This reaction had been introduced in 1986<sup>36</sup> and optimized successively<sup>37,38</sup> by Frauenrath et al. Recently, very high enantioselectivities using diphosphane-modified NiHal<sub>2</sub> complexes as catalysts were obtained.<sup>38</sup>

The standard reaction was carried out in a THF/methanol (2:1) mixture in the ratio catalyst:NaBH<sub>4</sub>:substrate = 1:26:200 at room temperature (reaction time 24 h).<sup>39</sup> Nitrogen was blown over the solution for 15 min to remove the hydrogen, which was formed from NaBH<sub>4</sub> and methanol. This reduced the amount of the hydrogenation product C to normally 1–2.5% (Table 4). The activity and stereoselectivity of ( $\eta^6$ -arene)ruthenium half-sandwich complexes **1–11** depended strongly on the arene ligand, the chiral salicylaldimine ligand, and the metal atom. The results are shown in Table 4.

(33) Frauenrath, H.; Runsink, J.; Scharf, H.-D. *Chem. Ber.* **1982**, *115*, 2728.

(34) Frauenrath, H.; Philipps, T. *Liebigs Ann. Chem.* **1985**, 1303.

(35) Frauenrath, H.; Philipps, T. *Liebigs Ann. Chem.* **1985**, 1951.

(36) Frauenrath, H.; Philipps, T. *Angew. Chem.* **1986**, *98*, 261; *Angew. Chem., Int. Ed. Engl.* **1986**, *25*, 274.

(37) Frauenrath, H.; Reim, S.; Wiesner, A. *Tetrahedron: Asymmetry* **1998**, *9*, 1103.

(38) Frauenrath, H.; Brethauer, D.; Reim, S.; Maurer, M.; Raabe, G. *Angew. Chem.* **2001**, *113*, 176; *Angew. Chem., Int. Ed.* **2001**, *40*, 177.

(39) Brunner, H.; Prommesberger, M. *Tetrahedron: Asymmetry* **1998**, *9*, 3231.

To analyze the influence of the arene ligand, complexes **1** and **9–11** were tested as catalysts. Quantitative conversion under standard reaction conditions was achieved only with complex **1**, which had served as the standard catalyst for the desymmetrization reaction before (entry 1).<sup>39</sup> Going from benzene via mesitylene to hexamethylbenzene in complexes **9–11** made the catalytic activity drop appreciably (entries 2–4). Whereas complexes **9** and **11** gave only low enantioselectivities of 3–5% ee, complex **10** afforded 20% ee, leaving the standard system **1** with 51% ee unrivaled.

The standard system **1** is derived from the commercially available (*S*)-1-phenylethylamine. A comparison with complexes **2** and **3**, derived from the amines (*S*)-1-(1-naphthyl)ethylamine and (*S*)-1-cyclohexylethylamine, commercially available as well, showed high conversion with an improved selectivity (entries 5 and 6). The equilibrium diastereomer ratios had increased from the phenyl derivative **1** (86:14) to the naphthyl derivative **2** (>99:1) and dropped to the cyclohexyl derivative **3** (54:46), showing that there is no parallelism to the catalytic reaction of Scheme 4. The (*S*)-leucinol derivative **4** (entry 7) gave low conversion, maybe because of tridentate ligand binding through the additional OH substituent and a disappointing enantioselectivity.

The change to salicylaldimine ligands derived from amino acid esters, such as the (*S*)-valine methyl ester derivative **HLL\*<sup>-</sup>5**, brought an appreciable improvement. In fact, complex **5** afforded enantioselectivities up to 64.3% ee with 98% conversion (entry 8), the best results ever obtained in the desymmetrization of 2-*n*-butyl-4,7-dihydro-1,3-dioxepin (A) using (arene)ruthenium half-sandwich complexes as catalysts. The iodo complex **12** (entry 9) gave almost the same results as the chloro complex **5**, whereas the enantioselectivity dropped for the valine benzyl ester derivative **6** (entry 10). Complexes **7** and **8**, which contained racemized ligands, showed very good to reasonable catalytic activities (98% and 63% conversion, respectively) but due to their racemic ligands no enantioselectivity (entries 11 and 12).

The variation of the transition metal resulted in another interesting result. In the above screening, ligands **HLL\*<sup>-</sup>1** and **HLL\*<sup>-</sup>5** had given the best results in ruthenium complexes. Using the same ligands in the corresponding osmium complexes, the catalytic activity decreased and, surprisingly, the enantioselectivity dis-

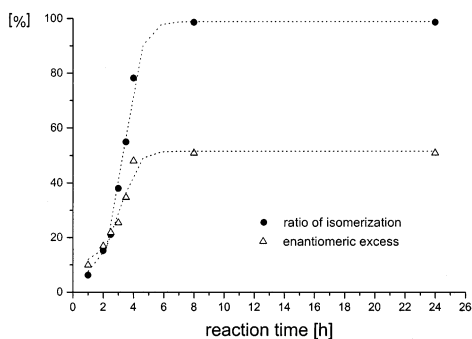


**Figure 3.** Conversion and enantiomeric excess of the isomerization product **B** as a function of time for the catalysis of Scheme 4.

appeared completely (entries 13 and 14). There is no explanation for this behavior.

In a study of the solvent dependence of the olefin isomerization according to Scheme 4, an "alcohol problem" had been encountered. If methanol in the standard solvent mixture THF/methanol was replaced by ethanol (or other alcohols), the enantioselectivity disappeared.<sup>39</sup> In the present study we confirmed this result with complex **5** as the catalyst. Under standard conditions using THF/ethanol (2:1) instead of THF/methanol (2:1), the catalytic activity dropped to about 60% conversion, the amount of hydrogenation product reached a maximum of 21%, and the enantioselectivity vanished.<sup>9</sup>

To investigate the reaction kinetics of the catalysis of Scheme 4, complex **1** (124 mg, 0.25 mmol) was dissolved in 30 mL of THF/methanol (2:1) and activated with NaBH<sub>4</sub> (250 mg, 6.60 mmol). Then 2-*n*-butyl-4,7-dihydro-1,3-dioxepin (**A**; 8.60 mL, 50.0 mmol) was added. In defined time intervals 3 mL was taken from the reaction mixture and worked up as described in the Experimental Section. Figure 3 shows the rise of yield and enantiomeric excess of the isomerization product **B** as a function of time.

After a period of slower reaction rate in the first 1–2 h, the yield of isomerization product **B** increased almost linearly. After 5–6 h conversion was quantitative. Using linear regression between 2.5 and 5 h the reaction rate was calculated as  $37.6 \pm 2.2 \text{ h}^{-1}$ . The time dependence of the enantiomeric excess showed the same sigmoidal curve as the conversion (Figure 3). There was an increase of the enantiomeric excess during the reaction, and values around 50% ee were only obtained at the end of the reaction. Usually, the enantiomeric excess is constant during a reaction. The increase observed here will allow an improvement of the enantioselectivity, in particular, after the mechanism of the catalysis has been established.

### Experimental Section

**General Remarks.** All manipulations and reactions, including metal compounds, were carried out under an inert atmosphere of dry nitrogen using standard Schlenk techniques. Most of the commercially available reagents were used without further purification. Solvents were dried by standard methods and distilled prior to use. Melting points: Büchi SMP 20, not corrected. IR spectra: Beckman IR 4240 spectrometer (KBr pellets). Mass spectra: Finnigan MAT 311 A (EI, electron impact method) and Finnigan MAT 95 (FD, field desorption method). Optical rotations: Perkin-Elmer 241 polarimeter at room temperature. <sup>1</sup>H NMR spectra: Bruker AC 250 spec-

trometer (250 MHz) and Bruker ARX 400 spectrometer (400 MHz). Elemental analyses: Elementar Vario EL III. X-ray structural analyses: STOE-IPDS diffractometer (Mo K $\alpha$  radiation, 173 K (Oxford Cryosystems Cooler,<sup>40</sup> graphite monochromator), SIR-97<sup>41</sup> and SHELXL-97.<sup>42</sup> [( $\eta^6$ -*p*-cymene)RuCl<sub>2</sub>]<sub>2</sub>, [( $\eta^6$ -benzene)RuCl<sub>2</sub>]<sub>2</sub>, [( $\eta^6$ -mesitylene)RuCl<sub>2</sub>]<sub>2</sub>, [( $\eta^6$ -hexamethylbenzene)RuCl<sub>2</sub>]<sub>2</sub>, and [( $\eta^6$ -*p*-cymene)OsCl<sub>2</sub>]<sub>2</sub> were prepared as published.<sup>43–47</sup>

**Preparation of Compounds HLL\*–1–HLL\*–8.** All the chiral salicylaldimines, except **HLL\*–3** and **HLL\*–6**, which were new compounds, were synthesized according to the literature.<sup>48–53</sup>

**(S)-(+)-(1-Cyclohexylethyl)salicylaldimine (HLL\*–3).** Salicylaldehyde (2.10 mL, 2.44 g, 20.0 mmol) was dissolved in 5 mL of methanol, and (*S*)-(1-cyclohexylethyl)amine (2.89 mL, 2.50 g, 19.6 mmol) was added. The mixture was heated to 55–60 °C for 2 h. The solvent was removed, and the oily residue was distilled under reduced pressure, giving a slightly yellow liquid. Yield: 3.82 g (84%). Bp: 113–115 °C/2 Torr. IR (neat):  $\nu$  3030 w, 2940 m, 2900 s, 2820 m (C–H), 1610 s (C=N), 1560 m (C=C). <sup>1</sup>H NMR (250 MHz, CDCl<sub>3</sub>, TMS):  $\delta$  1.25 (d, <sup>3</sup>J = 6.4 Hz, 3H, CH<sub>3</sub>), 1.82–0.86 (min, 11H, H cyclohexyl), 3.09 (dq, <sup>3</sup>J = <sup>3</sup>J = 6.4 Hz, 1H, =NCH), 6.86 (ddd, <sup>3</sup>J = 7.7 Hz, <sup>3</sup>J = 7.2 Hz, <sup>4</sup>J = 1.1 Hz, 1H, Sal H4), 6.98–6.93 (min, 1H, Sal H6), 7.33–7.21 (m, 2H, Sal H3, Sal H5), 8.27 (s, 1H, N=CH), 13.82 (bs, 1H, OH). MS (EI, 70 eV): *m/z* (relative intensity) 231 (54) [M], 148 (100), 121 (23). [ $\alpha$ ]<sub>D</sub> (c = 1.30, EtOH): +372°. Anal. Calcd for C<sub>15</sub>H<sub>21</sub>NO (231.3): C, 77.88; H, 9.15; N, 6.05. Found: C, 77.60; H, 9.12; N, 5.98.

**(S)-(+)-N-[1-(1-((Benzyloxy)carbonyl)-2-methylpropyl)]-salicylaldimine (HLL\*–6).** The salt (*S*)-benzyl valinate/*p*-toluenesulfonic acid<sup>54</sup> (5.65 g, 14.9 mmol) was suspended in 100 mL of methanol, and NaOMe (805 mg, 14.9 mmol) was added. To the resulting clear solution was added dropwise salicylaldehyde (156 mL, 1.82 g, 14.9 mmol), and the mixture was stirred at 55–60 °C for about 30 min. After it was cooled to room temperature, the yellow solution was stirred for 16 h. The solvent was removed. The residue was dissolved in 50 mL of CH<sub>2</sub>Cl<sub>2</sub> and the solution washed three times with 70 mL of water. The organic layer was dried over Na<sub>2</sub>SO<sub>4</sub>, and the solvent was removed. Adding 50 mL of petroleum ether to the yellow oil and cooling to –30 °C resulted in the formation of light yellow needles. Yield: 2.68 g (58%). Mp: 52–53 °C. IR (KBr, cm<sup>-1</sup>):  $\nu$  3040 w, 2970 m, 2880 m (C–H), 1730 w (C=O), 1630 vs (C=N), 1580 m (C=C). <sup>1</sup>H NMR (250 MHz, CDCl<sub>3</sub>, TMS):  $\delta$  0.94 (d, <sup>3</sup>J = 6.8 Hz, 3H, CH(CH<sub>3</sub>)<sub>2</sub>), 0.95 (d, <sup>3</sup>J = 6.8 Hz, 3H, CH(CH<sub>3</sub>)<sub>2</sub>), 2.39 (dsept, <sup>3</sup>J = 6.2 Hz, <sup>3</sup>J = 6.8 Hz, 1H, CH(CH<sub>3</sub>)<sub>2</sub>), 3.76 (d, <sup>3</sup>J = 6.2 Hz, 1H, =NCH), 5.20 (s, 2H, OCH<sub>2</sub>-Ph), 6.89 (ddd, <sup>3</sup>J = 7.7 Hz, <sup>3</sup>J = 7.2 Hz, <sup>4</sup>J = 1.1 Hz, 1H, Sal

(40) Cosier, J.; Glazer, A. M. *J. Appl. Crystallogr.* **1986**, *19*, 105.

(41) Altomare, A.; Casciarano, G.; Giacovazzo, C.; Guagliardi, A. *J. Appl. Crystallogr.* **1993**, *26*, 343.

(42) Sheldrick, G. M. SHELXL-97, Program for Crystal Structure Refinement; University of Göttingen, Göttingen, Germany, 1997.

(43) Winkhaus, G.; Singer, H.; Kricke, M. *Z. Naturforsch.* **1966**, *21B*, 11.09.

(44) Winkhaus, G.; Singer, H. *J. Organomet. Chem.* **1967**, *7*, 487.

(45) Bennett, M. A.; Huang, T. N.; Matheson, T. W.; Smith, A. K. *Inorg. Synth.* **1982**, *21*, 74.

(46) Bennett, M. A.; Smith, A. K. *J. Chem. Soc., Dalton Trans.* **1974**, *2*, 233.

(47) Werner, H.; Zenkert, K. *J. Organomet. Chem.* **1988**, *345*, 151.

(48) Smith, H. E.; Cook, S. C.; Warren, M. E. *J. Org. Chem.* **1964**, *29*, 2265.

(49) Warren, M. E.; Smith, H. E. *J. Am. Chem. Soc.* **1965**, *87*, 1757.

(50) Desimoni, G.; Fajta, G.; Mellerio, G.; Righetti, P. P.; Zanelli, C. *Gazz. Chim. Ital.* **1992**, *122*, 269.

(51) Grigg, R.; Gunaratne, H. Q. N.; Sridharan, V. *Tetrahedron* **1987**, *43*, 5887.

(52) Grigg, R.; Gunaratne, H. Q. N.; Kemp, J. *J. Chem. Soc., Perkin Trans. 1* **1984**, 41.

(53) Amomraksa, K.; Grigg, R.; Nimal Gunaratne, H. Q.; Kemp, J.; Sridharan, V. *J. Chem. Soc., Perkin Trans. 1* **1987**, 2285.

(54) Zervas, L.; Winitz, M.; Greenstein, J. P. *J. Org. Chem.* **1957**, *22*, 1515.



*HA*), 7.01–6.96 (m, 1H, *Sal H6*), 7.39–7.24 (m, 7H, *CH<sub>2</sub>Ph*, *Sal H3*, *Sal H5*), 8.31 (s, 1H, N=CH), 13.14 (bs, 1H, *OH*). MS (EI, 70 eV): *m/z* (relative intensity) 311 (59) [M], 176 (83) [*M* – CO<sub>2</sub>CH<sub>2</sub>Ph], 91.1 (100) [CH<sub>2</sub>Ph]. [ $\alpha$ ]<sub>D</sub> (*c* = 1.03, CH<sub>2</sub>Cl<sub>2</sub>): +1.36°. Anal. Calcd for C<sub>19</sub>H<sub>21</sub>NO<sub>3</sub> (311.4): C, 73.29; H, 6.80, N, 4.50. Found: C, 73.07; H, 7.17; N, 4.50.

**Preparation of the Complexes [( $\eta^6$ -arene)Ru(LL\*Cl)].** [( $\eta^6$ -*p*-cymene)Ru(LL\*-1)Cl] (**1**) and [( $\eta^6$ -benzene)Ru(LL\*-1)-Cl] (**9**) were synthesized according to the literature.<sup>25</sup> The novel complexes were synthesized using the following general procedure: 2.10 mmol of the appropriate ligand **HLL\*-1–HLL\*-8** was dissolved in 20 mL of absolute CH<sub>2</sub>Cl<sub>2</sub>, and KO<sup>t</sup>Bu (2.10 mmol) was added at room temperature. The mixture was stirred for 30 min. After the suspension was cooled to –78 °C, 1.00 mmol of [( $\eta^6$ -arene)RuCl<sub>2</sub>]<sub>2</sub> was added. The solution was stirred for 16 h, in the course of which the reaction mixture was warmed to room temperature. The volume of the solution was reduced to 50%. The solution was filtered over a short column loaded with Celite and SiO<sub>2</sub>. The purification of the crude product is specified for the individual complexes.

**[( $\eta^6$ -*p*-cymene)Ru(LL\*-2)Cl] (**2**).** Recrystallization was carried out from CH<sub>2</sub>Cl<sub>2</sub>/ether/hexane. Yield: 864 mg (79%), Mp: 212 °C dec. IR (KBr, cm<sup>-1</sup>):  $\nu$  3040 w, 2950 m, 2860 w (C–H), 1610 s, 1590 m (C=N). <sup>1</sup>H NMR (250 MHz, CDCl<sub>3</sub>, TMS; signals of the minor diastereomer are given in parentheses when different from those of the major diastereomer):  $\delta$  0.95 (d, <sup>3</sup>*J* = 6.9 Hz, 3H, CH<sub>3</sub><sup>Pr</sup>), 1.08 (d, <sup>3</sup>*J* = 6.9 Hz, 3H, CH<sub>3</sub><sup>Pr</sup>), 1.88 (d, <sup>3</sup>*J* = 7.0 Hz, 3H, CH<sub>3</sub>), 2.03 (s, 3H, CH<sub>3</sub> *p*-cymene), 2.63 (sept, <sup>3</sup>*J* = 6.9 Hz, 1H, CH<sup>Pr</sup>), 5.05/4.23 (AB, <sup>3</sup>*J* = 5.5 Hz, 2H, *H p*-cymene), 5.23/4.68 (AB, <sup>3</sup>*J* = 5.5 Hz, 2H, *H p*-cymene), 6.50 (ddd, <sup>3</sup>*J* = 7.9 Hz, <sup>3</sup>*J* = 6.7 Hz, <sup>4</sup>*J* = 1.0 Hz, 1H, *Sal HA*), 6.75 (q, <sup>3</sup>*J* = 7.0 Hz, 1H, =NCH), 7.01 (d, <sup>3</sup>*J* = 8.5 Hz, 1H, *Sal H6*), 7.08 (dd, <sup>3</sup>*J* = 7.9 Hz, <sup>4</sup>*J* = 1.8 Hz, 1H, *Sal H3*), 7.22 (ddd, <sup>3</sup>*J* = 8.5 Hz, <sup>3</sup>*J* = 6.7 Hz, <sup>4</sup>*J* = 1.8 Hz, 1H, *Sa H5*), 7.74–7.55 (m, 4H, *H naphthyl*), 8.02–7.89 (m, 2H, *H naphthyl*), 8.12 (s, 1H, N=CH), 8.22 (d, 1H, <sup>3</sup>*J* = 8.3 Hz, *H naphthyl*). MS (FD, CH<sub>2</sub>Cl<sub>2</sub>): *m/z* (relative intensity) 545 (100) [*M*] relative to <sup>102</sup>Ru. [ $\alpha$ ]<sub>D</sub> (*c* = 0.05, CH<sub>2</sub>Cl<sub>2</sub>): –180°. Anal. Calcd for C<sub>29</sub>H<sub>30</sub>ClNO<sub>3</sub>Ru (545.9): C, 63.81; H, 5.54; N, 2.57. Found: C, 64.16; H, 5.44; N, 2.41.

**[( $\eta^6$ -*p*-cymene)Ru(LL\*-3)Cl] (**3**).** Precipitation was carried out with petroleum ether from a CH<sub>2</sub>Cl<sub>2</sub> solution. Yield: 170 mg (17%). Mp: 81–83 °C dec. IR (KBr, cm<sup>-1</sup>):  $\nu$  3080 w, 2940 s, 2920 w, 2870 m (C–H), 1625 s, 1605 m (C=N). <sup>1</sup>H NMR (250 MHz, CDCl<sub>3</sub>, TMS; signals of the minor diastereomer are given in parentheses when different from those of the major diastereomer):  $\delta$  = 1.13 (1.15) (d, <sup>3</sup>*J* = 7.0 Hz, 3H, CH<sub>3</sub><sup>Pr</sup>), 1.27 (1.26) (d, <sup>3</sup>*J* = 7.0 Hz, 3H, CH<sub>3</sub><sup>Pr</sup>), 1.42–0.87 (m, 5H, *H cyclohexyl*), 1.48 (1.49) (d, <sup>3</sup>*J* = 6.8 Hz, 3H, CH<sub>3</sub>), 2.09–1.59 (m, 6H, *H cyclohexyl*), 2.17 (2.21) (s, 3H, CH<sub>3</sub> *p*-cymene), 2.82 (sept, <sup>3</sup>*J* = 7.0 Hz, CH(CH<sub>3</sub>)<sub>2</sub>), 4.39–4.15 (m, 1H, =NCH), 5.45–4.93 (m, 4H, *H p*-cymene), 6.41 (6.39) (ddd, <sup>3</sup>*J* = 7.8 Hz, <sup>3</sup>*J* = 6.8 Hz, <sup>4</sup>*J* = 1.1 Hz, 1H, *Sal HA*), 6.98–6.85 (m, 2H, *Sal H3*, *Sal H6*), 7.19–7.10 (m, 1H, *Sal H5*), 7.69 (7.60) (s, 1H, N=CH). MS (FD, CH<sub>2</sub>Cl<sub>2</sub>): *m/z* (relative intensity) 501 (100) [*M*] relative to <sup>102</sup>Ru. [ $\alpha$ ]<sub>D</sub> (*c* = 0.10, CH<sub>2</sub>Cl<sub>2</sub>): –160°. Anal. Calcd for C<sub>25</sub>H<sub>34</sub>ClNO<sub>3</sub>Ru (501.1): C, 59.93; H, 6.84; N, 2.80. Found: C, 60.53; H, 7.03; N, 2.84.

**[( $\eta^6$ -*p*-cymene)Ru(LL\*-4)Cl] (**4**).** Recrystallization was carried out from CH<sub>2</sub>Cl<sub>2</sub>/ether/hexane. Yield: 113 mg (12%), Mp: 153 °C dec. IR (KBr, cm<sup>-1</sup>):  $\nu$  3600–3100 m (O–H), 3010 w, 2930 s, 2900 m, 2840 w (C–H), 1600 s, 1580 m (C=N). <sup>1</sup>H NMR (250 MHz, CDCl<sub>3</sub>, TMS; signals of the minor diastereomer are given in parentheses when different from those of the major diastereomer):  $\delta$  1.18–1.06 (m, 9H, CH<sub>3</sub><sup>Pr</sup>, CH<sub>2</sub>CH(CH<sub>3</sub>)<sub>2</sub>), 1.26 (d, <sup>3</sup>*J* = 7.0 Hz, 3H, CH<sub>3</sub><sup>Pr</sup>), 1.94–1.72 (min, 3H, CH<sub>2</sub>CH(CH<sub>3</sub>), CH<sub>2</sub>OH), 2.25 (s, 3H, CH<sub>3</sub> *p*-cymene), 2.76 (sept, <sup>3</sup>*J* = 7.0 Hz, 1H, CH<sup>Pr</sup>), 3.74–3.61 (m, 1H, CH<sub>2</sub>CH(CH<sub>3</sub>)<sub>2</sub>), 4.09–3.91 (m, 2H, CH<sub>2</sub>OH), 4.65–4.53 (m, 1H, =NCH), 5.00 (d, <sup>3</sup>*J* = 5.5 Hz, 1H, *H p*-cymene), 5.53–5.41 (m, 3H, *H p*-cymene), 6.43 (ddd, <sup>3</sup>*J* = 7.8 Hz, <sup>3</sup>*J* = 6.8 Hz, <sup>4</sup>*J* = 1.1 Hz,

1H, *Sal HA*), 7.00–6.89 (m, 2H, *Sal H3*, *Sal H6*), 7.18 (ddd, <sup>3</sup>*J* = 8.6 Hz, <sup>3</sup>*J* = 6.8 Hz, <sup>4</sup>*J* = 1.6 Hz, 1H, *Sal H5*), 7.76 (7.85) (s, 1H, N=CH). MS (FD, CH<sub>2</sub>Cl<sub>2</sub>): *m/z* (relative intensity) 491 (100) [*M*] relative to <sup>102</sup>Ru. [ $\alpha$ ]<sub>D</sub> (*c* = 0.06, CH<sub>2</sub>Cl<sub>2</sub>): –1000°. Anal. Calcd for C<sub>23</sub>H<sub>32</sub>ClNO<sub>2</sub>Ru (491.0): C, 56.26; H, 6.57; N, 2.85. Found: C, 56.23; H, 6.47; N, 2.74.

**[( $\eta^6$ -*p*-cymene)Ru(LL\*-5)Cl] (**5**).** Recrystallization was carried out from toluene/petroleum ether. Yield: 486 mg (96%). Mp: 136 °C dec. IR (KBr, cm<sup>-1</sup>):  $\nu$  3060 w, 2980 m, 2890 w (C–H), 1750 s, 1730 s (C=O), 1625 s (C=N). <sup>1</sup>H NMR (250 MHz, CDCl<sub>3</sub>, TMS; signals of the minor diastereomer are given in parentheses when different from those of the major diastereomer):  $\delta$  1.01 (1.08) (d, <sup>3</sup>*J* = 6.5 Hz, 3H, CH(CH<sub>3</sub>)<sub>2</sub>), 1.04 (1.13) (d, <sup>3</sup>*J* = 6.5 Hz, 3H, CH(CH<sub>3</sub>)<sub>2</sub>), 1.09 (1.23) (d, *J* = 7.0 Hz, 3H, CH(CH<sub>3</sub>)<sub>2</sub> *p*-cymene), 1.21 (1.27) (d, <sup>3</sup>*J* = 7.0 Hz, 3H, CH(CH<sub>3</sub>)<sub>2</sub> *p*-cymene), 2.15 (2.22) (s, 3H, CH<sub>3</sub> *p*-cymene), 2.42 (dsept, <sup>3</sup>*J* = 10.1 Hz, <sup>3</sup>*J* = 6.5 Hz, 1H, CH(CH<sub>3</sub>)<sub>2</sub>), 2.77 (2.65) (sept, <sup>3</sup>*J* = 7.0 Hz, 1H, CH(CH<sub>3</sub>)<sub>2</sub> *p*-cymene), 3.90 (3.73) (s, 3H, OCH<sub>3</sub>), 4.80 (4.61) (d, <sup>3</sup>*J* = 10.1 (11.3) Hz, 1H, =NCH), 5.14 (5.02) (d, <sup>3</sup>*J* = 5.5 Hz, 1H, *H p*-cymene), 5.43–5.33 (m, 3H, *H p*-cymene), 6.43 (6.42) (ddd, <sup>3</sup>*J* = 7.8 Hz, <sup>3</sup>*J* = 6.8 Hz, <sup>4</sup>*J* = 1.1 Hz, 1H, *Sal HA*), 7.01–6.91 (m, 2H, *Sal H3*, *Sal H6*), 7.17 (7.16) (ddd, <sup>3</sup>*J* = 8.6 Hz, <sup>3</sup>*J* = 6.8 Hz, <sup>4</sup>*J* = 1.9 Hz, 1H, *Sal H5*), 7.95 (8.03) (s, 1H, N=CH). MS (FD, CH<sub>2</sub>Cl<sub>2</sub>): *m/z* (relative intensity) 505 (100) [*M*] relative to <sup>102</sup>Ru. [ $\alpha$ ]<sub>D</sub> (*c* = 0.16, CH<sub>2</sub>Cl<sub>2</sub>): +316°. Anal. Calcd for C<sub>23</sub>H<sub>30</sub>ClNO<sub>3</sub>Ru (505.0): C, 54.70; H, 5.99; N, 2.77. Found: C, 54.60; H, 6.06; N, 2.79.

**[( $\eta^6$ -*p*-cymene)Ru(LL\*-6)Cl] (**6**).** Recrystallization from CH<sub>2</sub>Cl<sub>2</sub>/petroleum ether. Yield: 395 mg (68%), Mp: 56 °C dec. IR (KBr, cm<sup>-1</sup>):  $\nu$  3040 w, 2970 m, 2940 w, 2880 w (C–H), 1740 s, (C=O), 1620 s (C=N). <sup>1</sup>H NMR (250 MHz, CDCl<sub>3</sub>, TMS; signals of the minor diastereomer are given in parentheses when different from those of the major diastereomer):  $\delta$  0.97 (1.04) (d, <sup>3</sup>*J* = 6.9 Hz, 3H, CH(CH<sub>3</sub>)<sub>2</sub> *p*-cymene), 1.01 (1.23) (d, <sup>3</sup>*J* = 6.6 Hz, 3H, CH(CH<sub>3</sub>)<sub>2</sub>), 1.02 (1.24) (d, <sup>3</sup>*J* = 6.6 Hz, 3H, CH(CH<sub>3</sub>)<sub>2</sub>), 1.13 (1.11) (d, <sup>3</sup>*J* = 6.9 Hz, 3H, CH(CH<sub>3</sub>)<sub>2</sub> *p*-cymene), 2.02 (2.18) (s, 3H, CH<sub>3</sub> *p*-cymene), 2.42 (dsept, <sup>3</sup>*J* = 10.1 Hz, <sup>3</sup>*J* = 6.6 Hz, 1H, CH(CH<sub>3</sub>)<sub>2</sub>), 2.68 (2.78) (sept, <sup>3</sup>*J* = 6.9 Hz, 1H, CH(CH<sub>3</sub>)<sub>2</sub> *p*-cymene), 4.78 (4.65) (d, <sup>3</sup>*J* = 10.1 (11.1) Hz, 1H, =NCH), 5.43–4.96 (m, 4H, *H p*-cymene), 5.43/5.25 (AB, <sup>2</sup>*J* = 11.8 Hz, 2H, CH<sub>2</sub>Ph), 6.43 (6.42) (ddd, <sup>3</sup>*J* = 7.8 Hz, <sup>3</sup>*J* = 6.8 Hz, <sup>4</sup>*J* = 1.0 Hz, 1H, *Sal HA*), 7.01–6.90 (m, 2H, *Sal H3*, *Sal H6*), 7.17 (7.18) (ddd, <sup>3</sup>*J* = 8.7 Hz, <sup>3</sup>*J* = 6.8 Hz, <sup>4</sup>*J* = 1.9 Hz, 1H, *Sal H5*), 7.51–7.31 (m, 5H, CH<sub>2</sub>Ph), 7.96 (8.06) (s, 1H, N=CH). MS (FD, CH<sub>2</sub>Cl<sub>2</sub>): *m/z* (relative intensity) 581 (100) [*M*] relative to <sup>102</sup>Ru. [ $\alpha$ ]<sub>D</sub> (*c* = 0.11, CH<sub>2</sub>Cl<sub>2</sub>): +202°. Anal. Calcd for C<sub>29</sub>H<sub>34</sub>ClNO<sub>3</sub>Ru (581.1): C, 59.94; H, 5.90; N, 2.41. Found: C, 59.33; H, 5.85; N, 2.20.

**[( $\eta^6$ -*p*-cymene)Ru(LL\*-7)Cl] (**7**).** Recrystallization was carried out from toluene/petroleum ether. Yield: 235 mg (42%). Mp: 169 °C dec. IR (KBr, cm<sup>-1</sup>):  $\nu$  3040 w, 2980 m, 2930 w (C–H), 1750 s (C=O), 1620 s (C=N). <sup>1</sup>H NMR (250 MHz, CDCl<sub>3</sub>, TMS; signals of the minor diastereomer are given in parentheses when different from those of the major diastereomer):  $\delta$  1.11 (0.92) (d, <sup>3</sup>*J* = 6.9 Hz, 3H, CH<sub>3</sub><sup>Pr</sup>), 1.19 (1.13) (d, <sup>3</sup>*J* = 6.9 Hz, 3H, CH<sub>3</sub><sup>Pr</sup>), 2.17 (2.05) (s, 3H, CH<sub>3</sub> *p*-cymene), 2.77 (2.57) (sept, <sup>3</sup>*J* = 6.9 Hz, 1H, CH<sup>Pr</sup>), 3.20 (dd, <sup>2</sup>*J* = 12.6 Hz, <sup>3</sup>*J* = 11.4 Hz, CH<sub>2</sub>Ph), 3.57 (dd, <sup>2</sup>*J* = 12.6 Hz, <sup>3</sup>*J* = 3.2 Hz, CH<sub>2</sub>Ph), 3.78 (3.73) (s, 3H, OCH<sub>3</sub>), 5.49–4.65 (m, 5H, *H p*-cymene, =NCH), 6.46 (6.47) (ddd, <sup>3</sup>*J* = 7.9 Hz, <sup>3</sup>*J* = 6.8 Hz, <sup>4</sup>*J* = 1.1 Hz, 1H, *Sal HA*), 7.02–6.92 (m, 2H, *Sal H3*, *Sal H6*), 7.48–7.09 (m, 6H, *Ph H*, *Sal H5*), 8.06 (8.28) (s, 1H, N=CH). MS (FD, CH<sub>2</sub>Cl<sub>2</sub>): *m/z* (relative intensity) 553 (100) [*M*] relative to <sup>102</sup>Ru. [ $\alpha$ ]<sub>D</sub> (*c* = 0.10, CH<sub>2</sub>Cl<sub>2</sub>): +40.2°. Anal. Calcd for C<sub>27</sub>H<sub>30</sub>ClNO<sub>3</sub>Ru (553.1): C, 58.64; H, 5.47; N, 2.53. Found: C, 58.33; H, 5.34; N, 2.36.

**[( $\eta^6$ -*p*-cymene)Ru(LL\*-8)Cl] (**8**).** Recrystallization was carried out from toluene/petroleum ether. Yield: 420 mg (78%), Mp: 158 °C dec. IR (KBr, cm<sup>-1</sup>):  $\nu$  3040 w, 2980 m, 2880 w (C–H), 1745 s (C=O), 1620 s (C=N). <sup>1</sup>H NMR (250 MHz, CDCl<sub>3</sub>, TMS; signals of the minor diastereomer are given in

parentheses when different from those of the major diastereomer):  $\delta$  1.10 (1.09) (d,  $^3J = 6.8$  Hz, 3H,  $CH_3$   $\text{Pr}$ ), 1.23 (d,  $^3J = 6.8$  Hz, 3H,  $CH_3$   $\text{Pr}$ ), 2.18 (2.15) (s, 3H,  $CH_3$   $p$ -cymene), 2.83 (sept,  $^3J = 6.8$  Hz, 1H,  $CH$   $\text{Pr}$ ), 4.02 (3.77) (s, 3H,  $OCH_3$ ), 5.11 (4.98) (d,  $^3J = 5.5$  Hz, 1H,  $H$   $p$ -cymene), 5.31 (d,  $^3J = 5.5$  Hz, 1H,  $H$   $p$ -cymene), 5.46 (d,  $^3J = 5.5$  Hz, 1H,  $H$   $p$ -cymene), 5.51 (d,  $^3J = 5.5$  Hz, 1H,  $H$   $p$ -cymene), 6.46–6.31 (m, 1H, Sal  $H4$ ), 6.67 (s, 1H,  $=NCH$ ), 7.00–6.72 (m, 2H, Sal  $H3$ , Sal  $H6$ ), 7.13 (ddd,  $^3J = 8.6$  Hz,  $^3J = 6.8$  Hz,  $^4J = 1.7$  Hz, 1H, Sal  $H5$ ), 7.55–7.28 (m, 6H, Ph  $H$ ,  $N=CH$ ). MS (FD,  $CH_2Cl_2$ ):  $m/z$  (relative intensity) 539 (100) [M] relative to  $^{102}Ru$ .  $[\alpha]_D$  ( $c = 0.11$ ,  $CH_2Cl_2$ ): +18.3°. Anal. Calcd for  $C_{26}H_{28}ClNO_3Ru$  (539.0): C, 57.93; H, 5.24; N, 2.60. Found: C, 57.93; H, 5.08; N, 2.47.

**$[(\eta^6\text{-mesitylene})Ru(LL^*-1)Cl]$  (10).** Recrystallization was carried out from  $CH_2Cl_2$ /hexane. Yield: 348 mg (72%). Mp: 172 °C dec. IR (KBr,  $cm^{-1}$ ):  $\nu$  3030 w, 2980 w, 2930 w (C–H), 1620 s, 1600 m (C=N).  $^1H$  NMR (250 MHz,  $CDCl_3$ , TMS; signals of the minor diastereomer are given in parentheses when different from those of the major diastereomer):  $\delta$  1.72 (d,  $^3J = 7.2$  Hz, 3H,  $CH(CH_3)$ ), 1.96 (2.14) (s, 9H,  $C_6H_3(CH_3)_3$ ), 4.68 (4.7 Hz) (s, 3H,  $C_6H_3(CH_3)_3$ ), 5.78 (5.56) (q,  $^3J = 7.2$  Hz, 1H,  $=NCH$ ), 6.49 (6.42) (ddd,  $^3J = 7.7$  Hz,  $^3J = 6.9$  Hz,  $^4J = 1.2$  Hz, 1H, Sal  $H4$ ), 7.07–6.83 (m, 2H, Sal  $H3$ , Sal  $H6$ ), 7.19 (7.15) (ddd,  $^3J = 8.5$  Hz,  $^3J = 6.9$  Hz,  $^4J = 1.8$  Hz, 1H, Sal  $H5$ ), 7.61–7.23 (m, 5H, Ph  $H$ ), 8.02 (s, 1H,  $N=CH$ ). MS (FD,  $CH_2Cl_2$ ):  $m/z$  (relative intensity) 481 (100) [M] relative to  $^{102}Ru$ .  $[\alpha]_D$  ( $c = 0.04$ ,  $CH_2Cl_2$ ): –485°. Anal. Calcd for  $C_{24}H_{26}ClNO_3Ru$  (481.0): C, 59.93; H, 5.45; N, 2.91. Found: C, 59.46; H, 5.47; N, 2.83.

**$[(\eta^6\text{-hexamethylbenzene})Ru(LL^*-1)Cl]$  (11).** Recrystallization was carried out from  $CH_2Cl_2$ /hexane. Yield: 115 mg (22%). Mp: 198 °C dec. IR (KBr,  $cm^{-1}$ ):  $\nu$  3040 w, 3000 w, 2900 w (C–H), 1600 s, 1580 m (C=N).  $^1H$  NMR (250 MHz,  $CDCl_3$ , TMS; signals of the minor diastereomer are given in parentheses when different from those of the major diastereomer):  $\delta$  1.82 (d,  $^3J = 7.1$  Hz, 3H,  $CH_3$ ), 1.96 (2.03) (s, 18H,  $C_6(CH_3)_6$ ), 5.59 (5.47) (q,  $^3J = 7.1$  Hz, 1H,  $CH$ ), 6.37 (ddd,  $^3J = 7.7$  Hz,  $^3J = 6.8$  Hz,  $^4J = 1.2$  Hz, 1H, Sal  $H4$ ), 6.85 (dd,  $^3J = 7.7$  Hz,  $^4J = 1.8$  Hz, 1H, Sal  $H3$ ), 6.96 (d,  $^3J = 8.6$  Hz, 1H, Sal  $H6$ ), 7.14 (ddd,  $^3J = 8.6$  Hz,  $^3J = 6.8$  Hz,  $^4J = 1.8$  Hz, 1H, Sal  $H5$ ), 7.49–7.30 (m, 5H, Ph  $H$ ), 7.73 (s, 1H,  $N=CH$ ). MS (FD,  $CH_2Cl_2$ ):  $m/z$  (relative intensity) 523 (100) [M] relative to  $^{102}Ru$ .  $[\alpha]_D$  ( $c = 0.06$ ,  $CH_2Cl_2$ ): –157°. Anal. Calcd for  $C_{27}H_{32}ClNO_3Ru$  (523.1): C, 62.00; H, 6.17; N, 2.68. Found: C, 61.86; H, 6.23; N, 2.84.

**$[(\eta^6\text{-}p\text{-cymene})Ru(LL^*-5)I]$  (12).** Complex **5** (90.0 mg, 0.18 mmol) was dissolved in 20 mL of absolute MeOH, and NaI (270 mg, 180 mmol) was added. The mixture was stirred for 3 h at room temperature. The solvent was evaporated, and the residue was dissolved in  $CH_2Cl_2$  and filtered through Celite. Removing the solvent yielded the analytically pure dark red powder **12**. Yield: 99.6 mg (94%). Mp: 160 °C dec. IR (KBr,  $cm^{-1}$ ):  $\nu$  2980 m, 2880 w (C–H), 1745 s (C=O), 1620 s (C=N).  $^1H$  NMR (250 MHz,  $CDCl_3$ , TMS; signals of the minor diastereomer are given in parentheses when different from those of the major diastereomer):  $\delta$  1.03 (1.08) (d,  $^3J = 6.5$  Hz, 3H,  $CH(CH_3)_2$ ), 1.09 (1.15) (d,  $^3J = 6.9$  Hz, 3H,  $CH(CH_3)_2$   $p$ -cymene), 1.16 (1.22) (d,  $^3J = 6.5$  Hz, 3H,  $CH(CH_3)_2$ ), 1.26 (1.31) (d,  $^3J = 6.9$  Hz, 3H,  $CH(CH_3)_2$   $p$ -cymene), 2.30 (2.38) (s, 3H,  $CH_3$   $p$ -cymene), 2.50 (dsept,  $^3J = 9.6$  Hz,  $^3J = 6.5$  Hz, 1H,  $CH(CH_3)_2$ ), 2.93 (2.91) (sept,  $^3J = 6.9$  Hz, 1H,  $CH(CH_3)_2$   $p$ -cymene), 3.90 (3.75) (s, 3H,  $OCH_3$ ), 4.79 (4.52) (d,  $^3J = 9.6$  Hz, 1H,  $=NCH$ ), 5.70–4.91 (m, 4H,  $H$   $p$ -cymene), 6.43 (6.42) (ddd,  $^3J = 7.9$  Hz,  $^3J = 6.8$  Hz,  $^4J = 1.1$  Hz, 1H, Sal  $H4$ ), 7.00–6.85 (m, 2H, Sal  $H3$ , Sal  $H6$ ), 7.16 (7.15) (ddd,  $^3J = 8.6$  Hz,  $^3J = 6.8$  Hz,  $^4J = 1.9$  Hz, 1H, Sal  $H5$ ), 7.78 (7.93) (s, 1H,  $N=CH$ ). MS (FD,  $CH_2Cl_2$ ):  $m/z$  (relative intensity) 597 (100) [M] relative to  $^{102}Ru$ .  $[\alpha]_D$  ( $c = 0.10$ ,  $CH_2Cl_2$ ): +507°. Anal. Calcd for  $C_{23}H_{30}ClNO_3Ru$  (596.5): C, 46.31; H, 5.07; N, 2.35. Found: C, 45.98; H, 5.10; N, 2.25.

**Preparation of the Complexes  $[(\eta^6\text{-}p\text{-cymene})Os(LL^*)\text{-Cl}]$ .** The osmium complexes were synthesized as described

above for the corresponding ruthenium complexes using 0.50 mmol of  $[(\eta^6\text{-}p\text{-cymene})OsCl_2]_2$  and 1.00 mmol of the respective ligand.

**$[(\eta^6\text{-}p\text{-cymene})Os(LL^*-1)Cl]$  (13).** Recrystallization was carried out from toluene/ $CH_2Cl_2$ /petroleum ether. Yield: 245 mg (84%), Mp: 190–195 °C dec. IR (KBr,  $cm^{-1}$ ):  $\nu$  3060 w, 3020 w, 2960 m, 2820 w (C–H), 1615 s (C=N).  $^1H$  NMR (250 MHz,  $CDCl_3$ , TMS; signals of the minor diastereomer are given in parentheses when different from those of the major diastereomer):  $\delta$  1.06 (1.18) (d,  $^3J = 6.9$  Hz, 3H,  $CH_3$   $\text{Pr}$ ), 1.20 (1.29) (d,  $^3J = 6.9$  Hz, 3H,  $CH_3$   $\text{Pr}$ ), 1.81 (1.84) (d,  $^3J = 7.0$  Hz, 3H,  $CH_3$ ), 2.23 (2.25) (s, 3H,  $CH_3$   $p$ -cymene), 2.56 (2.72) (sept,  $^3J = 6.9$  Hz, 1H,  $CH$   $\text{Pr}$ ), 5.89–5.23 (min, 5H,  $=NCH$ ,  $H$   $p$ -cymene), 6.46 (6.38) (ddd,  $^3J = 7.8$  Hz,  $^3J = 6.8$  Hz,  $^4J = 1.0$  Hz, 1H, Sal  $H4$ ), 7.01–6.75 (m, 2H, Sal  $H3$ , Sal  $H6$ ), 7.73–7.17 (m, 6H, Ph  $H$ , Sal  $H5$ ), 7.91 (7.66) (s, 1H,  $N=CH$ ). MS (FD,  $CH_2Cl_2$ ):  $m/z$  (relative intensity) 585 (100) [M] relative to  $^{192}Os$ .  $[\alpha]_D$  ( $c = 0.10$ ,  $CH_2Cl_2$ ): +48°. Anal. Calcd for  $C_{25}H_{28}ClNO_3Os$  (584.2): C, 51.40; H, 4.83; N, 2.40. Found: C, 51.82; H, 4.83; N, 2.43.

**$[(\eta^6\text{-}p\text{-cymene})Os(LL^*-5)Cl]$  (14).** Recrystallization was carried out from toluene/petroleum ether. Yield: 184 mg (62%), Mp: 115 °C dec. IR (KBr,  $cm^{-1}$ ):  $\nu$  3060 w, 2970 m, 2880 w (C–H), 1730s (C=O), 1610 s (C=N).  $^1H$  NMR (250 MHz,  $CDCl_3$ , TMS; signals of the minor diastereomer are given in parentheses when different from those of the major diastereomer):  $\delta$  1.02 (1.04) (d,  $^3J = 6.7$  Hz, 3H,  $CH(CH_3)_2$ ), 1.10 (1.14) (d,  $^3J = 7.0$  Hz, 3H,  $CH(CH_3)_2$   $p$ -cymene), 1.15 (d,  $^3J = 6.7$  Hz, 3H,  $CH(CH_3)_2$ ), 1.24 (1.28) (d,  $^3J = 7.0$  Hz, 3H,  $CH(CH_3)_2$   $p$ -cymene), 2.24 (2.30) (s, 3H,  $CH_3$   $p$ -cymene), 2.48 (dsept,  $^3J = 10.3$  Hz,  $^3J = 6.7$  Hz, 1H,  $CH(CH_3)_2$ ), 2.63 (2.64) (sept,  $^3J = 7.0$  Hz, 1H,  $CH(CH_3)_2$   $p$ -cymene), 3.85 (3.74) (s, 3H,  $OCH_3$ ), 4.76 (4.52) (d,  $^3J = 10.3$  (11.2) Hz, 1H,  $=NCH$ ), 5.50 (5.39) (d,  $^3J = 5.4$  Hz, 1H,  $H$   $p$ -cymene), 5.88–5.63 (m, 3H,  $H$   $p$ -cymene), 6.47 (ddd,  $^3J = 7.9$  Hz,  $^3J = 6.7$  Hz,  $^4J = 1.1$  Hz, 1H, Sal  $H4$ ), 6.91–6.85 (m, 1H, Sal  $H6$ ), 7.07–7.03 (m, 1H, Sal  $H3$ ), 7.25 (7.26) (ddd,  $^3J = 8.6$  Hz,  $^3J = 6.7$  (6.9) Hz,  $^4J = 1.9$  Hz, 1H, Sal  $H5$ ), 8.05 (8.14) (s, 1H,  $N=CH$ ). MS (FD,  $CH_2Cl_2$ ):  $m/z$  (relative intensity) 595 (100) [M] relative to  $^{192}Os$ .  $[\alpha]_D$  ( $c = 0.10$ ,  $CH_2Cl_2$ ): +308°. Anal. Calcd for  $C_{23}H_{30}ClNO_3Os$  (594.2): C, 46.50; H, 5.09; N, 2.36. Found: C, 46.36; H, 5.00; N, 2.40.

**Catalytic Double-Bond Isomerization.** The catalytic isomerizations were carried out under an atmosphere of dry nitrogen. The catalyst (0.025 mmol) was dissolved in 3 mL of THF/MeOH (2:1).  $NaBH_4$  (25.0 mg, 1.32 mmol) was added, followed by 0.86 mL (5.00 mmol) of 2-*n*-butyl-4,7-dihydro-1,3-dioxepin. To remove the developing hydrogen, a stream of nitrogen was passed over the solution for 15 min. After 24 h the reaction was stopped by bubbling air through the solution. The solvent was evaporated, and the oily residue was purified by distillation under reduced pressure (70 °C, 2–3 Torr). Conversion was determined by  $^1H$  NMR spectroscopy (250 MHz,  $CDCl_3$ ). The integrals of the following signals were used: starting material **A**, multiplet ( $\delta$  5.77–5.65 ppm); product **B**, doublet of doublets ( $\delta$  6.35 ppm); hydrogenation product **C**, multiplet ( $\delta$  3.93–3.55 ppm). The enantiomer analysis was carried out by gas chromatography: HP 5890 A, Restek Rt-P $\beta$ DEXcst column (30 m, 0.32 mm i.d.). Conditions: carrier gas  $H_2$ , 82 °C isothermal. Retention times: (–)-enantiomer of **B**, 15.2 min; (+)-enantiomer of **B**, 16.0 min; hydrogenation product **C**, 16.9 min; starting material **A**, 19.3 min.

**Supporting Information Available:** Figures and tables giving X-ray data for complexes **2**, **5**, **7**, **8**, and **12–14**, including atomic coordinates, displacement parameters, bond lengths and angles, hydrogen coordinates, and hydrogen bonds. This material is available free of charge via the Internet at <http://pubs.acs.org>.